

Comparative Analysis of Blockchain-based Smart Contracts for Solar Electricity Exchanges

Jason Lin, Manisa Pipattanasomporn, and Saifur Rahman
Bradley Department of Electrical and Computer Engineering
Advanced Research Institute, Virginia Tech
Arlington, VA, USA
jason.lin@vt.edu

Abstract—With the advent of blockchain technology and the increasing penetration of rooftop photovoltaic (PV) systems, a new opportunity for energy trading through smart contracts has emerged. Challenges arise in such transactive markets to ensure individual rationality, incentive compatibility, budget balance, and economic efficiency during the auction process. This paper presents a comparative analysis of different smart contracts for solar electricity exchange in terms of market demand and supply metrics. Auction mechanisms considered in this paper are discriminatory and uniform k-Double Auction (k-DA). A simulation case study of 100 participants in a microgrid is presented using typical residential load and solar PV generation profiles. Results indicate that the discriminatory k-DA mechanism has the highest average percentage of contracts cleared and quantity traded during the period of excess solar energy generation, regardless of the level of PV penetration.

Index Terms—auction mechanism, blockchain, double auction, smart contract, transactive energy

I. INTRODUCTION

With the declining price of renewable energy technologies and institution of green energy policies, the current utility sector is undergoing a transformation. Traditionally, the electricity market follows a hierarchical model dependent on the centralized authority of utility companies where power is generated. Due to the penetration of PV systems at the residential level, more and more electricity consumers are able to produce and sell excess energy – thus becoming prosumers.

However, the conventional architecture of utilities is restricted in scalability to distributed generation integration [1]. Thus, coordination mechanisms through a transactive energy (TE) system is essential for autonomous prosumers [2]. Authors in [3] define TE as “a system of economic and control mechanisms that allows the dynamic balance of supply and demand across the entire electrical infrastructure using value as a key operational parameter”. A novel approach to implementing a TE market is through peer-to-peer (P2P) energy trading on blockchain technology. With the use of a distributed ledger, cryptocurrency and smart contracts,

blockchains allow the autonomous operation of energy transactions to be fair, secure, and trustworthy without depending on a central clearinghouse.

Authors in [4] review current existing blockchain based P2P energy trading projects. The Brooklyn Microgrid is currently the only operating microgrid in the United States where neighbors can trade locally produced solar energy [5]. The Key2Energy concept provides cheaper electricity to tenants from self-generated PV energy in multi-apartment homes [6]. The Enerchain project targets P2P energy trading of wholesale electricity over blockchains [7]. While high level overviews pertaining to the business, legal, and financial matters of these projects are available, detailed technical implementations are not publicly accessible.

This paper reviews selected auction mechanisms to be applied to a TE market within a microgrid. Metrics are then presented for quantifying the economic efficiency of discriminatory and uniform k-DA mechanisms. A simulation case study of a 100 home microgrid with varying degrees of PV penetration is then discussed for analyzing the selected mechanisms for excess solar electricity exchange.

II. AUCTION MECHANISMS

Auction mechanisms serve as the core part of the TE market in which smart contracts are implemented. While a multitude of mechanisms exist, this section briefly explores several common mechanisms.

A. Discriminatory k-Double Auction (Discriminatory k-DA)

In k-DA [8], buyers submit sealed bids B^P while sellers submit sealed asks S^P . Following the natural ordering rule, bids are sorted in a descending order while asks are sorted in an ascending order. If $B^P \geq S^P$, a trade occurs at price p :

$$p = kB^P + (1 - k)S^P \quad (1)$$

where k is a predetermined constant in $[0, 1]$. A k value in $(0, 1)$ permits both buyers and sellers to influence the trading price. Since the trading price is determined between each

winning buyer-seller pair, the described mechanism is discriminatory. In this case, there is no single market clearing price at each auction interval; trading prices vary among different winning buyer-seller pairs.

B. Uniform k-Double Auction (Uniform k-DA)

The uniform k-DA mechanism is a variation to the discriminatory k-DA mechanism where trading price is uniform for all winning participants. Such market clearing price is determined by first finding the largest breakeven index γ where $B_\gamma^P \geq S_\gamma^P$. The market clearing price is then set as:

$$p = kB_\gamma^P + (1 - k)S_\gamma^P \quad (2)$$

where B_γ^P and S_γ^P are the bidding price and asking price at the largest breakeven index, respectively. This auction mechanism yields a single market clearing price at each auction interval.

C. Vickrey-Clark-Groves (VCG)

An alternative mechanism is the Vickrey-Clark-Groves (VCG) mechanism, which maximizes social welfare and motivates participants to bid truthfully at the expense of the market operator [9]. With this mechanism,

winning buyers pay:

$$p_B = \max(S_\gamma^P, B_{\gamma+1}^P) \quad (3)$$

sellers receive:

$$p_S = \min(S_{\gamma+1}^P, B_\gamma^P) \quad (4)$$

where $B_{\gamma+1}^P$ and $S_{\gamma+1}^P$ are the bidding price and asking price following the largest breakeven index, respectively. Due to the natural ordering rule for sorting offers, $B_\gamma^P \geq B_{\gamma+1}^P$. Similarly, $S_\gamma^P \leq S_{\gamma+1}^P$. Since $p_B \leq p_S$, there exists a deficit that needs to be subsidized by the market operator to facilitate the trade.

D. Trade Reduction (TR)

To avoid subsidization of trades yet maintain participants to bid truthfully, the Trade Reduction (TR) method limits trades to $\gamma - 1$ buyers and sellers [9]. Such differs from uniform k-DA and VCG, where γ buyers and sellers are allowed to transact. Because buyer γ and seller γ are not permitted to participate in TR, social welfare is not maximized. However, trading buyers pay B_γ^P and trading sellers receive S_γ^P . As $B_\gamma^P \geq S_\gamma^P$, the market operator may financially gain $B_\gamma^P - S_\gamma^P$ from each single unit transaction.

III. MECHANISM PROPERTIES

The following briefly explains four properties of an ideal market mechanism: individual rationality, budget balance, truthfulness, and economic efficiency [8]. However, the Myerson-Satterthwaite theorem proves that these four conditions cannot occur simultaneously [10].

A. Individual Rationality

In individual rationality, no agent shall lose from participating in the mechanism. Thus, $p \leq B^P$ and $p \geq S^P$, where p , B^P , and S^P are the trading price, bidding price, and asking price, respectively. All four previously discussed

mechanisms exhibit individual rationality as a trade only occurs when $B^P \geq S^P$.

B. Budget Balance

A budget balanced market ensures that the mechanism itself does not subsidize or gain from trades between buyers and sellers. Thus, payments by buyers must be the amount received by sellers. Both discriminatory and uniform k-DA mechanisms are budget balanced as trade prices net zero between buyers and sellers. The VCG mechanism is not budget balanced as subsidy is required. The TR method is considered weakly budget balanced as the mechanism may gain but not lose financially.

C. Truthfulness

Also called incentive compatibility or strategy-proofness, the mechanism must motivate participants to reveal their values truthfully. Thus, participants can ensure best outcomes when acting upon their true preferences. Both discriminatory and uniform k-DA mechanisms are not incentive compatible as buyers and sellers may submit lower and higher offers, respectively, for individual gain. However, VCG ensures truthful bidding as the ability to transact and the transaction price are determined by both buyers and sellers, shown in equations (3) and (4). TR is also incentive compatible as trading participants have no incentive to bid otherwise. Non-participating γ^{th} buyer and seller may submit offers better than $B_{\gamma-1}^P$ or $S_{\gamma-1}^P$, respectively. However, this will result in negative utilities.

D. Economic Efficiency

Economic efficiency maximizes sum of all individual utilities (social welfare). Thus, a limited quantity of goods is allocated to those who value them the most. Both k-DA and VCG mechanisms are economically efficient as no participants are precluded from the market. However, the TR mechanism forbids the γ^{th} buyer and seller from trading.

Based on the above criteria, discriminatory and uniform k-DA mechanisms are selected to support the TE market in this study. Both mechanisms do not require any subsidy to facilitate trades between buyers and sellers as in the case of VCG. In addition, k-DA does not preclude any participant from trading, as in the case of TR. Using the evaluation metrics defined below, effects of variations in both k-DA mechanisms are compared and analyzed.

IV. EVALUATION METRICS

The first three mechanism properties, i.e., individual rationality, budget balance, and incentive compatibility, are predetermined by the mechanism itself. However, the degree of economic efficiency has to be quantitatively analyzed. This study quantifies economic efficiency through three metrics: percentage of kWh sold, percentage of kWh bought, and percentage of households cleared. These are measured from the perspectives of sellers, buyers, and microgrid, respectively.

The metrics are calculated at each hourly auction interval during the availability of excess solar energy generation.

A. Percentage of kWh Sold

From the sellers' perspective, the percentage of kWh sold is defined as the ratio of the total kWh traded to the total kWh supplied for sales, as defined in (5). The higher the ratio, the higher sellers' PV outputs are successfully traded.

$$\sum_{m=1}^{N_T} T_m^Q / \sum_{j=1}^{N_S} S_j^Q \quad (5)$$

B. Percentage of kWh Bought

From the buyers' perspective, the percentage of kWh bought is defined as the ratio of the total kWh traded to the total kWh needed by the buyers, as defined in (6). The higher the ratio, the higher buyers' demands are met.

$$\sum_{m=1}^{N_T} T_m^Q / \sum_{i=1}^{N_B} B_i^Q \quad (6)$$

C. Percentage of Households Cleared

From the microgrid's perspective, the percentage of households cleared is the ratio of total participants whose orders have been completely filled, as defined in (7). Note the use of Iverson brackets, where the expression evaluates to 1 if true; 0 otherwise. B_i^Q and S_j^Q are updated upon each successful trade to reflect the quantities remaining to be purchased and sold, respectively.

$$\frac{\sum_{i=1}^{N_B} [B_i^Q = 0] + \sum_{j=1}^{N_S} [S_j^Q = 0]}{N_B + N_S} \quad (7)$$

Where,

- N_B, N_S, N_T : Total number of buyers, sellers and trades
- B_i^Q : kWh quantity demanded by buyer i
- S_j^Q : kWh quantity supplied by seller j
- T_m^Q : Total kWh quantity transacted for trade m

Together, the above three metrics form the basis for comparing discriminatory and uniform k-DA.

V. CASE STUDY DESCRIPTION

This study focuses on a microgrid of 100 homes in the Washington, D.C. metropolitan area. A typical single family home in this area is either single-story or two-stories tall, ranging from 1,000 to 4,000 square feet total. A uniform distribution of house sizes is created for the microgrid, with load profiles and PV production profiles generated using the methods explained below.

A. Load Profiles

The hourly load profile used in this study is obtained from the U.S. Department of Energy with data based on the Building America Housing Simulation B10 Benchmark [11]. This represents an average load profile for a typical home in the Washington, D.C. metropolitan area during the hottest summer month of August [12]. Shown in Fig. 1, the load profile represents an average house size of 2,546 square feet. This base load profile is scaled proportionally to the

previously generated home size. Additionally, a random $\pm 20\%$ deviation is introduced to induce variability.

B. PV Generation Profiles

The hourly PV generation profile is obtained from a 6.44kW PV system installed at the Virginia Tech Advanced Research Institute in Arlington, Virginia [13]. The system comprises of 28 x 230W PV panels with a total area of 485 square feet. Shown in Fig. 1, the PV generation profile represents a sunny day in the summer of July.

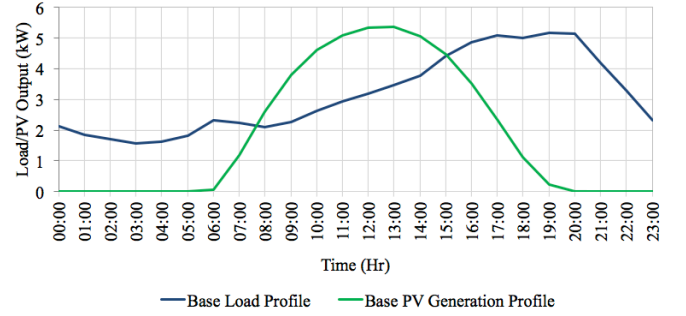


Fig. 1. A 24-hour load/PV generation profile.

The PV generation profile for each prosumer is determined by scaling the base PV generation profile to the size of usable roof space of each home. With each generated single home ranging from 1,000 to 4,000 square feet, foundation area is assumed to range from 1,000 to 2,000 square feet. All homes are assumed to have gable roofs (Fig. 2) with only one side available for PV installation. Conventional roof pitches (slopes) for residential homes range from $\tan \theta = [4/12, 9/12]$ [14]. Through reverse area projection, available roof space for PV installation can be determined by $A_{roof} = 0.5A_{foundation} \cos^{-1} \theta$. Additionally, it is assumed that approximately only $\sim 70\%$ of available roof space can be utilized for PV panels [15]. A random $\pm 20\%$ deviation is also introduced to vary hourly PV generation, thus accounting for variations in efficiency, tree shading, cloud coverage, etc.

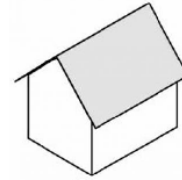


Fig. 2. Gable roof.

C. Simulation Scenarios

Fig. 3 illustrates the various scenarios that are simulated. For a microgrid of 100 homes, three different PV penetration levels are tested: 30%, 50%, and 70%. Offer prices from sellers and buyers at each hourly auction interval are sorted according to the natural ordering rule. Both discriminatory and uniform k-DA mechanisms are investigated with varying degrees of k values. In this study, the offer from each buyer is comprised of a bidding price and the kWh quantity to be purchased; the offer from each seller is comprised of an asking price and the kWh of excess PV generation to be sold. Bidding

and asking prices are randomly generated between \$0.01/kWh and \$1/kWh, inclusive. kWh quantities are based on the load/PV generation profiles as discussed previously.

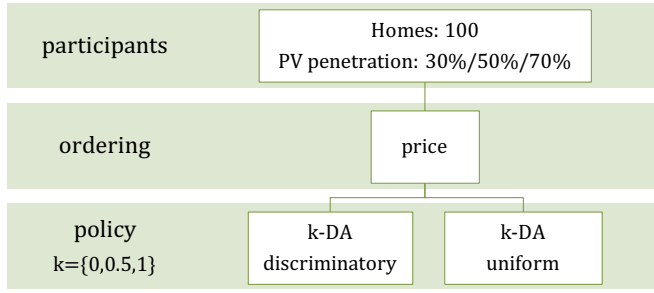


Fig. 3. Simulated scenarios.

VI. RESULTS AND DISCUSSION

Results are discussed below based on different penetration levels of prosumers in the microgrid.

A. Case I: 30% PV Penetration

Fig. 4 shows the 24-hour load and PV output profiles for a microgrid of 70 consumers and 30 prosumers. Note that the buyer demand profile is stacked on top of the seller demand profile to indicate total load of the microgrid. The total prosumer load is lower than the total consumer load due to the seller/buyer ratio. As shown, the peak load of this microgrid is ~550kW between the hours of 17:00 and 20:00.

With 30% PV penetration, the total PV capacity in this microgrid is 263.1kW; peak PV output is ~200kW at around 13:00. There is excess solar energy production from the prosumers between ~07:30 to 16:00 that can be traded among the neighbors in the microgrid.

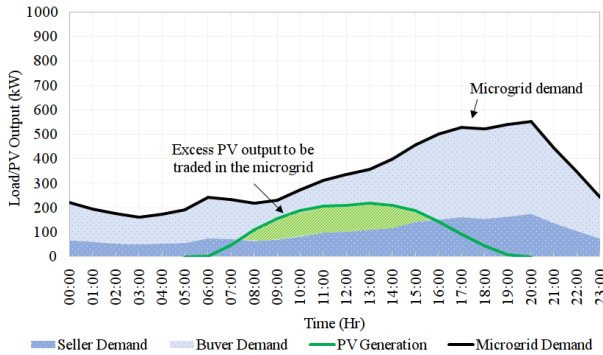


Fig. 4. Microgrid supply vs demand at 30% PV penetration level.

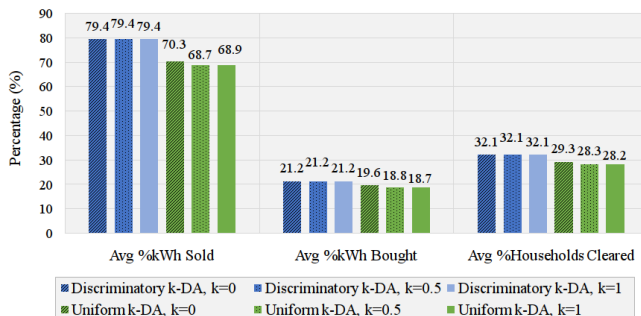


Fig. 5. Comparison of economic efficiencies at 30% PV penetration.

Results in Fig. 5 indicate that discriminatory k-DA offers higher average %kWh sold/bought and households cleared than those of the uniform k-DA. Varying degrees of k values do not affect trading outcomes for discriminatory k-DA, while those of uniform k-DA are slightly affected. This makes sense as the k value only affects the trading price between each winning buyer-seller pair, indicated in (1). However in uniform k-DA, the market clearing price is set by the breakeven index and varied by k , as in (2). Hence, transactions are limited to buyers whose offers are better than the clearing price. This results in lower economic efficiency for uniform k-DA compared to discriminatory k-DA.

B. Case II: 50% PV Penetration

Fig. 6 illustrates the load and PV generation profiles for the microgrid at 50% PV penetration. Similar to Case I, excess solar generation is available for trading from ~07:30 to 16:00. Due to the higher ratio of prosumers to consumers, there is an excess of PV output between ~08:30 to 13:30 from the microgrid even after total consumption by every home. While slightly lower due to randomness in profile generation, the peak load is still at around 500kW between ~16:00 and 20:00. The total prosumer load is approximately the same as the total consumer load due to the 50/50 seller/buyer ratio.

The total PV capacity in this scenario is 432.5kW; peak PV output is around 350kW at around 12:00. There is an excess of solar energy production from approximately 07:00 to 16:00 available for trade within the microgrid.

Results in Fig. 7 indicate the same generality as in Case I. Discriminatory k-DA leads to the highest average percentage of households whose orders are completely cleared, as well as %kWh sold and bought. Similarly, all three metrics are the same for discriminatory k-DA regardless of k values.

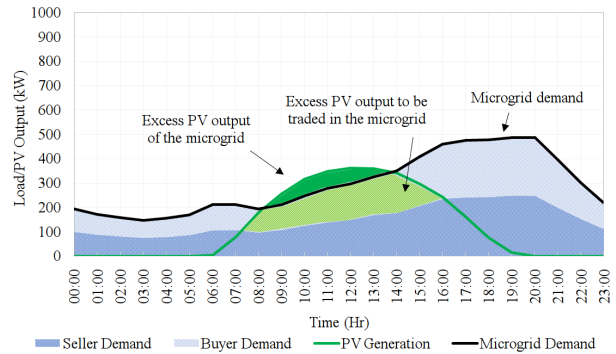


Fig. 6. Microgrid supply vs demand at 50% PV penetration level.

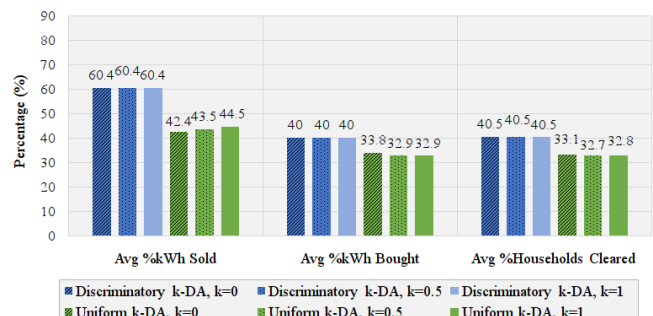


Fig. 7. Comparison of economic efficiencies at 50% PV penetration.

C. Case III: 70% PV Penetration

Fig. 8 illustrates the load and PV generation profiles for a microgrid of 30 consumers and 70 prosumers. As in Case II, there is an excess of PV energy between ~07:30 to 15:00 even after self consumption. Note that there is more demand from the sellers due to higher ratio of prosumers to consumers. However, the total peak load of 500kW between ~17:00 to 20:00 is consistent with the first two scenarios.

At 70% PV penetration, the total PV capacity in this microgrid is 638.4kW; peak PV output is ~550kW at around 12:00. Results in Fig. 9 indicate the same outcome pertaining to discriminatory k-DA as in Cases I and II.

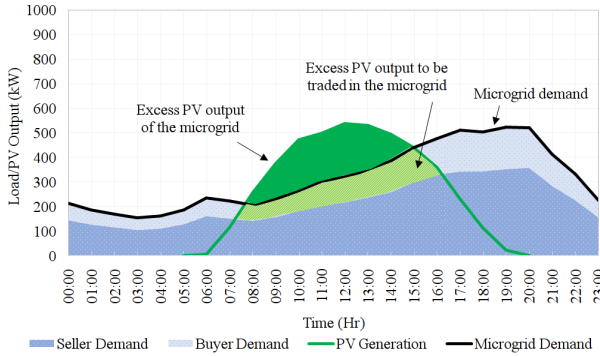


Fig. 8. Microgrid supply vs demand at 70% PV penetration level.

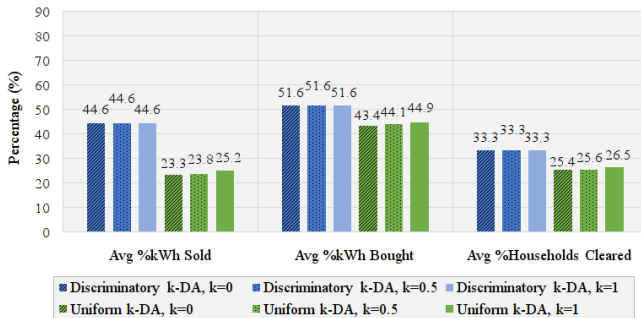


Fig. 9. Comparison of economic efficiencies at 70% PV penetration.

For all three levels of PV penetration, discriminatory k-DA outperforms uniform k-DA with respect to the defined economic efficiency indices: average percentage of kWh sold/bought and average percentage of households cleared.

With increasing PV penetration, average percentage of kWh sold decreases and average percentage of kWh bought increases. Such is valid as there is excess supply from prosumers with lower consumer demand. However, the metric for average percentage of households cleared is not only dependent on PV penetration levels, but also on consumer demand as well as bidding and asking prices. As prices are randomly generated via a uniform distribution, direct conclusions pertaining this metric may not be drawn. Nevertheless, it is important to note that during the ideal scenario of market equilibrium (where market supply equals market demand and asking prices equal bidding prices), all three economic efficiency metrics achieve 100%.

VII. CONCLUSION AND FUTURE WORK

This study explores different auction mechanisms that can facilitate an hour-ahead energy trading between residential consumers and prosumers within a microgrid of 100 homes. Three cases are simulated with different PV penetration levels, i.e., 30%, 50%, and 70% of homes with solar. Results indicate that regardless of PV market penetration, discriminatory k-DA outperforms uniform k-DA in all three economic efficiency indices: average percentage of kWh sold/bought and average percentage of households cleared. However due to changes in offer prices as well as market demand/supply, percentages of households cleared may vary greatly. Different mechanisms may be applied and combined to maximize economic efficiency. Thus, future work may be expanded to include multitude of auction mechanisms, different methods to determine bidding/asking prices, as well as buyer/seller ordering rules.

REFERENCES

- [1] M. Sabounchi and J. Wei, "Towards resilient networked microgrids: Blockchain-enabled peer-to-peer electricity trading mechanism," *2017 IEEE Conference on Energy Internet and Energy System Integration (EI2)*, Beijing, 2017, pp. 1-5.
- [2] A. Hahn, R. Singh, C.-C. Liu, and S. Chen, "Smart contract-based campus demonstration of decentralized transactive energy auctions," *2017 IEEE Power & Energy Society Innovative Smart Grid Technologies Conference (ISGT)*, 2017.
- [3] "GridWise Architecture Council," *GridWise Architecture Council*. [Online]. Available: www.gridwiseac.org. [Accessed: 04-Sep-2018].
- [4] A. Goranovic, M. Meisel, L. Fotiadis, S. Wilker, A. Treytl, and T. Sauter, "Blockchain applications in microgrids an overview of current projects and concepts," *IECON 2017 - 43rd Annual Conference of the IEEE Industrial Electronics Society*, 2017.
- [5] "Brooklyn Microgrid," *Brooklyn Microgrid*. [Online]. Available: <https://www.brooklyn.energy/>. [Accessed: 02-Sep-2018].
- [6] "Key2Energy: Accounting Locally Generated Photovoltaic Energy in Apartment Buildings," *guh GmbH*. [Online]. Available: <https://nynea.io/en/blog/key2energy-accounting-locally-generated-photovoltaic-energy-in-apartment-buildings>. [Accessed: 3-Sep-2018].
- [7] "Enerchain Project Overview and Key Insights," *Enerchain*. [Online]. Available: https://ponton.de/downloads/enerchain/EnerchainKeyInsights_2018-03-29_final.pdf. [Accessed: 03-Sep-2018].
- [8] D. C. Parkes, "Classic Mechanism Design." Available: www.eecs.harvard.edu/~parkes/pubs/ch2.pdf. [Accessed: 04-Sep-2018].
- [9] M. Babaioff and N. Nisan, "Concurrent auctions across the supply chain," *Proceedings of the 3rd ACM conference on Electronic Commerce - EC 01*, 2001.
- [10] M. A. Satterthwaite and S. R. Williams, "Bilateral trade with the sealed bid k-double auction: Existence and efficiency," *Journal of Economic Theory*, vol. 48, no. 1, pp. 107-133, 1989.
- [11] "Commercial and Residential Hourly Load Profiles for all TMY3 Locations in the United States," *Open Energy Information*. [Online]. Available: <https://openei.org/doe-opendata/dataset/commercial-and-residential-hourly-load-profiles-for-all-tmy3-locations-in-the-united-states>. [Accessed: 04-Sep-2018].
- [12] US Department of Commerce and NOAA, "DCA Normals, Means, and Extremes," *National Weather Service*, 11-Jun-2015. [Online]. Available: www.weather.gov/lwx/dcanme. [Accessed: 04-Sep-2018].
- [13] Virginia Tech Advanced Research Institute, "PV Generation Profile."
- [14] "Typical Roof Pitch," *MyRooff.com*. [Online]. Available: <https://myrooff.com/standart-roof-pitch/>. [Accessed: 22-Aug-2018].
- [15] "5 Things to consider before you plan for a rooftop PV plant," *Sustainability Outlook*. [Online]. Available: <http://www.sustainabilityoutlook.in/content/5-things-consider-you-plan-rooftop-pv-plant>. [Accessed: 05-Sep-2018].